SHAKE TABLE TEST OF A FULL-SCALE 10-STORY MASS TIMBER BUILDING WITH UPLIFT FRICTION DAMPERS

D.M. Dowden[1], A. Tatar[2]

[1] Michigan Technological University, Houghton, MI, United States, dmdowden@mtu.edu

[2] Michigan Technological University, Houghton, MI, United States

Abstract: *Self-centering Cross-Laminated Timber (SC-CLT) rocking walls have been established as a seismically resilient Seismic Force-Resisting Systems for mass timber buildings with high potential. The literature is rich in experimental studies that show that CLT walls exhibit essentially rigid rocking behaviour and require supplemental damping systems to dissipate energy during an earthquake. In this experimental study, the dynamic response of a recently introduced low-damage Uplift Friction Damper (UFD) for CLT rocking wall systems is investigated. Experimental tests were conducted as a separate payload project using the Natural Hazards Engineering Research Infrastructure (NHERI) TallWood full-scale 10-story mass timber building shake table test specimen. Tests were conducted at the NHERI Large High Performance Outdoor Shake Table at the University of California, San Diego. The results of this experimental test program phase with the UFDs are presented.*

1. Introduction

Cross-laminated timber (CLT) has recently emerged as an innovative construction material for mass-timber building construction within the United States (U.S.) and has also paved the way for other more recent mass timber panel products (e.g., mass panel plywood, dowel laminated, etc.). Benefits of these structural products include rapid construction, high strength-to-weight ratio, fire resistance, eco-sustainability, and low embodied carbon footprint (Green and Karsh 2012, Pei, van de Lindt et al. 2016). Of significance, CLT has provided a pathway for the potential of tall (i.e., 8 to 20 stories) mass-timber building alternatives that weren't possible before in the U.S., where traditional light framed timber structures are typically restricted to 5 to 6 stories maximum (Council 2015). In the U.S. tall mass timber buildings that use prescriptive design methods, currently require hybrid systems using mass timber panels to support only floor and roof gravity loads, whereby lateral seismic/wind forces are resisted by conventional lateral force resisting systems (LFRSs) constructed of steel and/or concrete. The latter underutilizes the full potential of CLT as a modern construction material. Recently, CLT shear wall seismic performance factors have been established for use as the first CLT-based SFRSs to be adopted in the U.S. building codes (van de Lindt, Amini et al. 2020). Although a significant achievement, the latter is still limited to buildings with six stories or less.

Barriers still exist that restrict the use of mass timber based seismic-force resisting systems (SFRSs) for tall buildings. This includes lack of appropriate CLT-specific seismic energy dissipation devices/connections and knowledge gaps in seismic performance of tall mass timber building systems subjected to dynamic earthquake loadings. Self-centering cross-laminated timber (SC-CLT) rocking walls have emerged as CLT-based SFRSs that show high promise in advancing mass timber technologies. Recent research has shown that SC-CLT rocking walls are feasible and have the benefit of being inherently seismically resilient compared to conventional code-based prescriptive SFRSs. Specifically, SC-CLTs can provide building self-centering and concentrates inelastic energy dissipation (damage) to replaceable elements (i.e., structural fuses). Unlike seismically resilient SFRSs, the inelastic energy dissipation elements of conventional SFRSs are coupled with the gravity frame system leading to irreparable structural damage and large residual building drifts remain after a moderate to large earthquake leaving the building vulnerable to possible collapse. Consequently, buildings with conventional SFRSs would likely face demolition after a large seismic event. This could have profound socio-economic crippling effects in heavily urbanized areas (Moehle, Barkley et al.). The 2010-2011 Christchurch earthquakes and the rebuilding of Christchurch (where buildings were designed with modern seismic codes, construction material, and practices) has highlighted this issue (Bruneau and MacRae 2017).

To advance knowledge of tall mass timber building systems towards practical implementation, as part of the NHERI TallWood project, the TallWood project team (Pei, van de Lindt et al. 2016) designed a large-scale 10-story mass timber building for testing at the NHERI outdoor shake-table at the University of California, San Diego (UCSD). This test is the first large-scale, tall mass-timber building shake-table test with SC-CLT rocking walls. These tests were completed in June 2023. This benchmark test program has validated the realization of tall mass-timber buildings with seismically resilient mass timber-based SFRSs. Based on the culmination of research established from the NHERI TallWood project leading up to these large-scale shake table tests (Pei, van de Lindt et al. 2019), the mass timber rocking wall SFRSs were detailed with U-shaped flexural steel plate (UFP) energy dissipators (Kelly, Skinner et al. 1972). Although the use of these dampers showed excellent performance, hysteretic yielding dampers have limitations including stiffness and strength degradation, and plastic strain accumulation that is the predominate root cause of large residual building drifts. Furthermore, although these hysteretic yielding dampers were shown to isolate controlled damage to the sacrificial elements detailed to be replaced, practical challenges could remain in replacing these elements post-seismic event. To overcome some of these limitations, this payload research project investigated a low-damage uplift friction damper (UFD) for mass timber rocking walls that provides stable energy dissipation, enhanced self-centering capabilities, and eliminates the need for repair/replacement of these devices post-seismic event. For this purpose, after the NHERI TallWood team completed their tests, UFDs were installed, and additional earthquake tests were conducted. This paper presents the experimental results and findings of these additional shake table tests to validate the performance of the proposed UFDs subjected to real simulated earthquakes on a test building with realistic boundary conditions.

2. Background

2.1 Review of Relevant Literature

An approach for providing seismic energy dissipation for SC-CLT walls has been the use of hysteretic metallic yielding structural fuses located at the foundation base of the wall (Smith, Ludwig et al. 2007, Kramer, Barbosa et al. 2016, Sarti, Palermo et al. 2016). These elements adopt similar principles as buckling-restrained-braces (BRB) used in conventional braced-frame SFRSs (ASCE 2017), which provide energy dissipation in both uniaxial tension and compression. An alternative approach has been the use of inter-panel shear connectors or coupled-walls (Iqbal, Pampanin et al. 2015, Sarti, Palermo et al. 2016, Akbas, Sause et al. 2017, Ganey, Berman et al. 2017). This approach was used by the NHERI project team for SC-CLT walls (Blomgren, Pei et al. 2019, Pei, van de Lindt et al. 2019, van de Lindt, Furley et al. 2019) and adopted for their NHERI TallWood 10-story building shake table tests. However, as with all yielding elements, inter-panel shear connectors are susceptible to strength and stiffness degradation and may need to be replaced post-event. Other forms of hysteretic metallic yielding dampers have been proposed (Polastri, Giongo et al. 2018, Trutalli, Marchi et al. 2019), but most are proprietary in nature and still inherently rely on inelastic damage. To overcome some of these limitations of hysteretic metallic yielding dampers in CLT-based SFRSs, others have investigated friction-based dampers that provide stable energy dissipation where repair is not expected post-event (Loo, Quenneville et al. 2016, Hashemi, Zarnani et al. 2018).

2.2 Uplift Friction Damper

The proposed uplift friction dampers (UFDs) are expected to provide stable energy dissipation, some self-centering capabilities, and friction plates easily replaceable after a design level seismic event if needed. Details of the proposed friction damper for a SC-CLT rocking wall is schematically shown in Figure 1. In that detail, energy dissipation is provided through abrasive friction from the relative sliding between two angled steel wedges. Here, one wedge is attached directly to the sides of the CLT wall (referenced as the “vertical” wedge). A second wedge is attached to a tension-rod bolted to the foundation that resists the uplift wall forces (referenced as the “horizontal” wedge). Note that the reference of the vertical and horizontal wedge refers to the motion of the wedges when the wall uplifts at the UFD locations due to wall rocking. That is the vertical wedge that is attached to the wall, moves primarily in the vertical direction with the wall. The horizontal wedge that is anchored to the uplift tension rod, moves primarily in the horizontal direction out-of-plane from the wall. The two wedges are clamped together with high strength thru-rods, where the wedge attached to the CLT wall is detailed with vertically slotted holes to accommodate the relative movement between the two wedges. The anchor tension-rods are detailed with pinned connections at each of its end to allow unrestrained rotation at these connection points allowing relative movement of the steel friction wedges. Connections of the damper to the CLT wall are provided through fully threaded self-tapping screws positioned at 45 degrees about the surface of the CLT panel. Out of plane stability for the CLT wall is provided by shear keys. Furthermore, shear keys are also provided in the in-plane direction to transfer the base shear to the foundation at the toes of the wall. Post-tensioned elements are provided at the mid-length of the wall to provide wall self-centering. In general, the kinematics of the UFDs is independent of the wall material type. That is with minor modifications the friction dampers could also be adapted for any rigid rocking wall system of any material.

The friction force generated in the damper is generated through a normal clamping force provided by the high strength rods in combination with stacked disc-washers (i.e., referred to as the bolt-disc spring element) as schematically presented in Figure 2. Some self-centering capability of this damper is provided through the detailing of an angled surface between the two contact surfaces of the sliding wedges in combination with the normal clamping force. This basic concept has been considered by others and shows high promise (Filiatrault, Tremblay et al. 2000, Hashemi, Zarnani et al. 2018). The bolt-disc spring element maintains a normal clamping force applied to the friction interface and represents a linear elastic spring of constant axial stiffness. While stacked disc-springs (e.g., Belleville washers) in series increase the total horizontal displacement of the horizontal wedge, stacking disc-springs in parallel will increase the clamping force of the bolt-disc spring component. The stacking configuration washers (i.e., parallel, series, or combination) will affect the stiffness of the bolt-disc spring component and provides the opportunity to “tune” the damper for a target performance. Considering the rocking motion of the CLT panel, the clamping force in the bolt-disc spring element increases by each increment of wall uplift to the point where all disc springs have reached their flatting force (which should be avoided in design). The condition where all washers are flattened is the maximum horizontal travel of the wedges representing the maximum uplift displacement condition of the vertical wedge and CLT wall. Analytical equations and detailed presentation describing the basic kinematics of the UFD have been established based on first principles using simplified free-body-diagrams (FBDs) and presented in (Tatar and Dowden 2022).

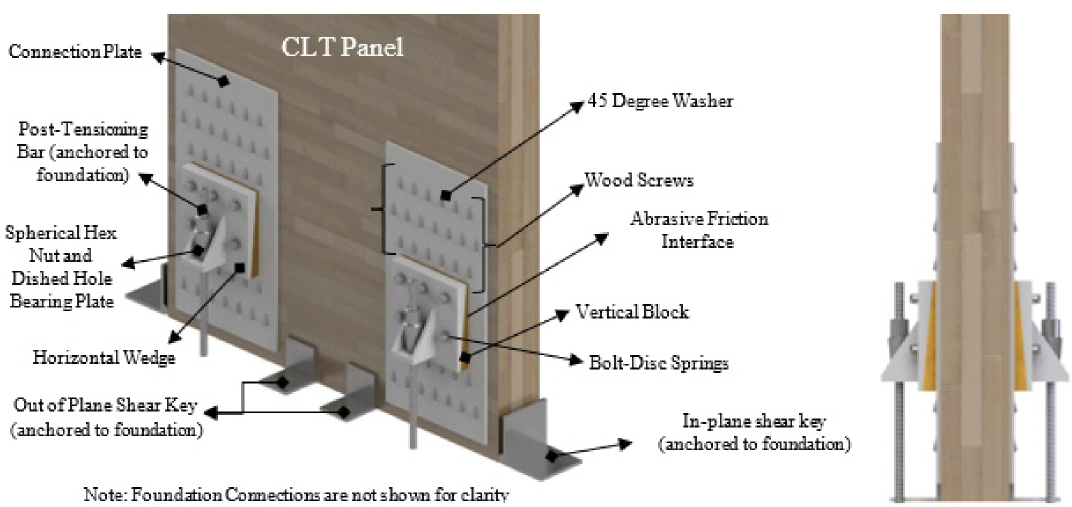

Figure 1. UFD components

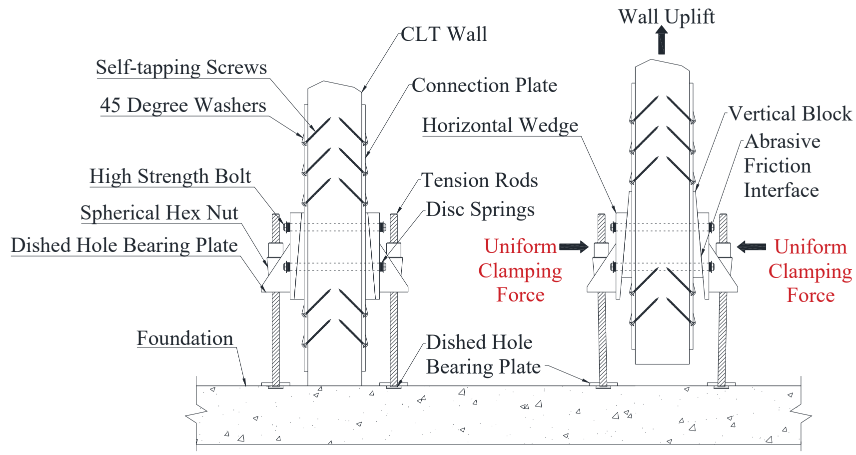

Figure 2. UFD Kinematics

3. Payload Shake Table Test Setup

3.1 NHERI TallWood 10-story mass timber building

The mass timber 10-story test building designed by the TallWood project team incorporated a variety of combinations of different mass timber products. The gravity frame system consisted of a beam-column grid with veneer laminated timber (VLT) beams and columns. The floor/roof panels utilized various panel types along the height of the building consisting of CLT, nail/dowel laminated timber, and VLT panels. The lateral system consisted of a pair of exterior post-tensioned rocking walls with VLT bounding columns in each orthogonal building direction (i.e., two rocking walls in each direction). The rocking walls in the North-South direction and East-West direction comprised of mass plywood panel (MPP) and CLT panels, respectively (see Figure 3 and Figure 4). Each of these rocking walls were post-tensioned with a total of four 32 mm (1.25 in.) diameter Simpson Strong-Tie ATS-HSR10 steel rods anchored at the foundation level and the tops of the wall at the roof level. An initial post-tensioning force of approximately 50% the yield strength of the PT rods was provided. Seismic energy dissipation was provided using U-flexural plate (UFP) steel yielding dampers detailed between the bounding column-to-wall connections at each level. The floor panels were sheathed with nailed plywood panels to transfer lateral forces to the rocking walls through diaphragm action. A detailed description and lateral seismic design of the 10-story building is presented by (Wichman, Berman et al. 2022, Pei, van de Lindt et al. 2023). Tests were conducted at the NHERI shake table located at University of California San Diego (i.e., NEHRI@UCSD).

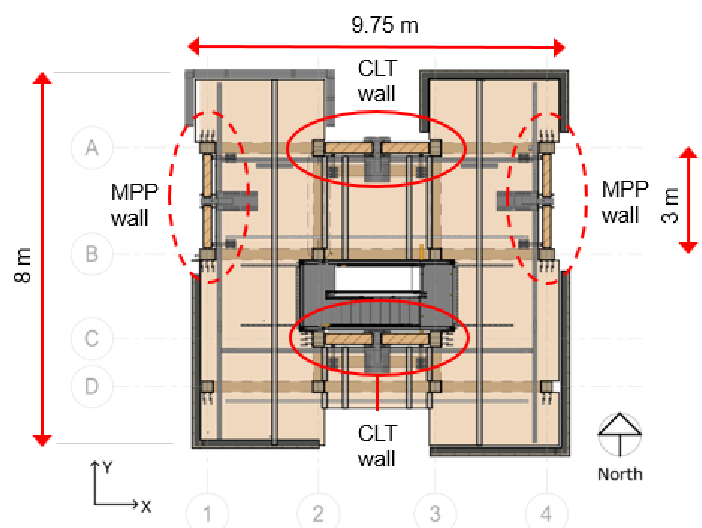

Figure 3. Post-tensioned rocking walls (image courtesy of NHERI TallWood)

(a) West MPP Wall (b) East MPP Wall

Figure 4. MPP wall elevations

3.2 MTU Payload Test with UFDs

The payload shake-table tests reported in this paper occurred after completion of the test program conducted by the NHERI TallWood project team. The objective of these payload tests was to validate the performance of the proposed UFDs subjected to simulated dynamic earthquake loads installed on rocking walls with realistic boundary conditions. Given the existing design constraints of the 10-story building constraints (previously established by the NHERI TallWood team), the UFDs were installed as added supplemental energy dissipation elements, while all other existing conditions of the test building remain unchanged. Furthermore, due to budgetary and time constraints, UFDs were installed on walls in only one primary direction. Since the UFDs were installed after the NHERI TallWood testing was finished, the MPP walls in the N-S direction were selected to avoid interference with the building's central stair core.

A 3D rendering of the fabricated UFDs is presented in Figure 5a. As highlighted in the figure, the UFDs comprise of two main components. The first components include the concrete filled hollow horizontal and vertical wedges fabricated with 12.7 mm (1/2 in.) thick Grade 345 MPa (50 ksi) steel plates. Plastic plugs were 3D printed and installed prior to the concrete filling providing hollow block outs for the thru-rods. Detailing the wedges as hollow steel shells with concrete fill reduces the damper weight and eliminates the need for solid thick steel plates. In particular, depending on the angle of inclination of the friction interface referenced from vertical and the overall size of the friction wedges, the use of solid steel wedges could become unpractical. For the dampers used in these tests, the angle of inclination referenced from a vertical axis of the inclined friction surface was 15 degrees. The vertical wedge is welded to the steel wall mounting plate and this assembly is attached to the MPP walls with Simpson Strong-Tie (SDCF221334) 45-degree oriented 8 mm x 349 mm (0.315 in. x 13.75 in.) self-tapping screws. The second components include the 25.4 mm (1 in.) diameter Simpson Strong-Tie ATS-HSR8 vertical anchor tension rods nested inside HSS76.2x6.35 (HSS3x0.25) steel pipe columns. In this assembly, the tension rods anchor the horizontal wedges to the foundation and the HSS steel pipe column supports the weight of the concrete filled steel horizontal wedges and ensures the horizontal wedges remain essentially at the same elevation as the vertical wedges slide against the horizontal wedges during wall rocking. Furthermore, the connections at the top and bottom of the pipe column/tension rod assemblies were attached to the foundation beam and the horizontal wedge with spherical plate washers to allow unrestrained rotation at these connection points.

Furthermore, the friction materials used 12.7 mm (1/2 in.) thick leaded-tin-bronze (LTB) and stainless steel (SS) plates. The LTB plates consisted of a C93200 alloy plate and was attached to the vertical wedges. The SS plate consisted of Type 410 plate and attached to the horizontal wedges. The friction plates were attached to the UFD wedges with 12.7 mm (½ in.)-13 threaded steel cap screws. The damper components on opposite faces of the MPP wall were tied together with 19 mm (3/4 in.) diameter Simpson Strong-Tie ATS-HSR6 tension thru-rods. To provide the clamping force needed to develop friction forces between the horizontal and vertical wedge interfaces, steel disc-washers (disc-springs) with a conical disc height to thickness ratio (h/t) of 0.57 were used at each end of the thru-rods. The stacking configuration consisted of a parallel series of 6 disc-washers stacked in parallel (i.e., nested) and each nested bundle placed in series 10 times. This stacking configuration provided an axial spring stiffness of approximately 175 kN/m (31.4 kip/in) per thru-rod. A finished installed damper is presented in Figure 5b shown at the exterior face of the West MPP wall.

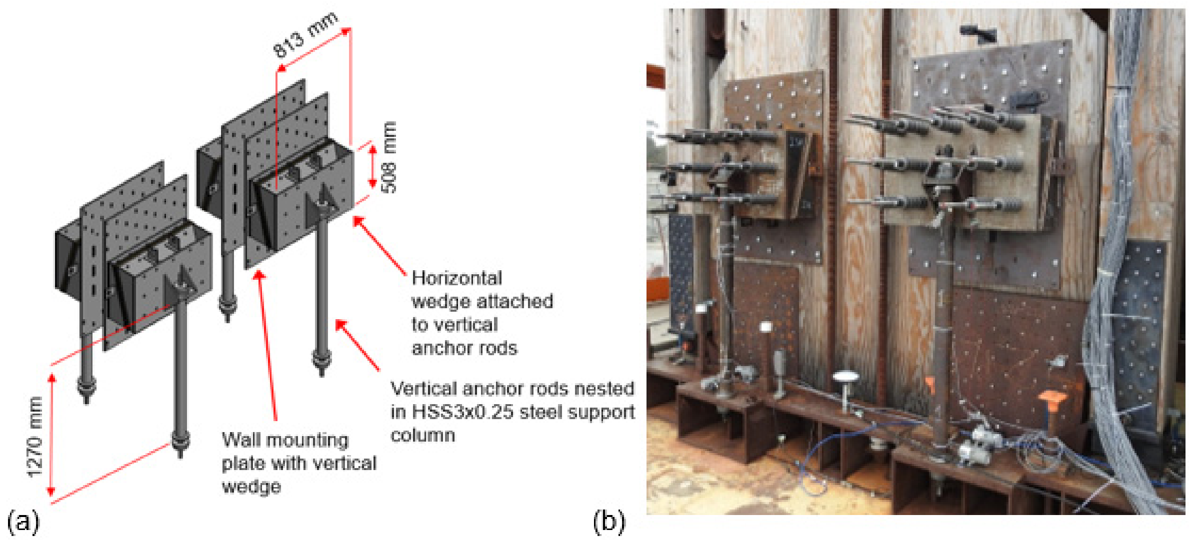

Figure 5. (a) UFD schematic; (b) Installed UFD at West MPP wall

As noted earlier, these tests are essentially a continuation of shake table testing beyond the NHERI TallWood project tests, but with UFDs installed at the base of the MPP rocking walls. Accordingly, all existing instrumentation from the NHERI TallWood team's tests were left in place and utilized for these tests. As such, for each UFD, 12 sensors were added at each damper location to monitor forces and displacements for a total of 48 additional instrumentation sensors added to the test building. Instrumentation sensors included load washers (i.e., load cells) at 5 of the 13 thru-rods per UFD, a load washer at each uplift tension rod, a vertical oriented string potentiometer at each horizontal and vertical wedge, and a horizontal oriented string potentiometer on the horizontal wedges located inside of the building. Lastly, with the instrumentation installed, the thru-rods were each post-tensioned to an initial rod clamping force ranging between approximately 13.3 to 22.2 kN (3 to 5 kips). All data collected by the instrumentation was collected at a sample rate of 256 Hz.

4. Loading Protocol and Select Experimental Results

4.1 Loading Protocol

The loading protocol consisted of 10 earthquake tests. Furthermore, to determine natural frequencies and quantify changes in dynamic properties of the building, white noise (i.e., an acceleration-controlled flat-spectrum broadband random motion) identification tests were also conducted. Given that these payloads tests are essentially an extension of the NHERI TallWood tests but with the added friction dampers installed, ground motion (GM) selections for the tests were based on a pre-defined suite of GMs established by and previously used by the NHERI TallWood team in their testing program. This was necessary since these GMs were already tuned for the shake table drive control and scaled to various target seismic hazard levels specific for the 10-story building design. A detailed presentation on the ground motion scaling and development of GMs used in these tests can be found at (Wichman, Berman et al. 2022). Furthermore, repeating select GMs used by the NHERI TallWood team also provided an opportunity to compare building response with and without the UFD dampers for a given earthquake test. For these tests, five different historical earthquake accelerograms were selected each with a different scaled seismic hazard (i.e., 225, 475, 975, and 2475 (MCE_R) year return periods). Because the UFDs were installed only in the North-South orientation (Y-direction), typically the earthquake tests were performed with only the Y-component (horizontal) or combination of the Y and Z (vertical) components of the accelerograms. For brevity, only results from the Loma Prieta ground motion are reported here, as this represents the MCE_R level scaled earthquake test leading to the most extreme demands on the test building.

4.2 Experimental Results – Global Response

The global response performance of the building is assessed by base shear, peak floor accelerations, and peak interstory drifts. Select response plots quantifying these parameters are presented in Figure 6 through Figure 7. The base shear was calculated as the summation of story forces that were obtained as the total acceleration response measured from accelerometers at each story level, multiplied by the approximate mass at that level. For this purpose, accelerometers installed at the approximate center of mass at each floor level were used to calculate these forces. Furthermore, the raw acceleration data was modified using a low-pass/high-pass filters retaining only frequency content between 0.1 Hz to 50 Hz. This frequency band was selected to ensure all dominant modes were included based on eigen analysis of the numerical model that informed that the fundamental mode was approximately 2 seconds (in the MPP Y-direction) and informed by the white-noise tests transfer functions that showed the dominant frequencies. Additionally, given the height of the test building, string potentiometers to measure floor level displacements could only be installed up to floor level 4. Consequently, floor/roof level displacements along the building height used to obtain the interstory drifts were calculated through numerical double integration of the response history data collected by the accelerometers. The global response data presented in Figure 6 through Figure 7 support the following observations:

1. The hysteretic response presented in Figure 6 provides an indicator of energy dissipation and global behavior. Furthermore, the peak base shear was determined to be approximately 899 kN (202 kips). The total seismic weight of the building was estimated at 2,615 kN (588 kips). Thus, the normalized base shear can be rewritten in terms of the gravity constant as 0.34g. Using this latter as a proxy for a base shear coefficient, in comparison to the ASCE7-16, this compares reasonably well to the spectral acceleration of 0.35g (at an approximate fundamental period of 2 seconds) from the code-based MCE_R horizontal response spectrum for which the NHERI TallWood team designed the test building.
2. The peak roof drift was measured to be 1.57%. This is below the 2% code drift limit. This observation in combination with item #1 above, provides support that the design methodology the NHERI TallWood team used to design the 10-story building satisfied these code-based design parameters.
3. An envelope of the min., max., and peak interstory drifts and accelerations are presented in Figure 7. The dashed lines represent the max. and mins., whereas the solid line with data point markers follows the absolute peaks along the height of the building. As observed, the peak interstory drift occurred at level 10 with a measured value of 2.33%. Furthermore, it is observed that the peak level acceleration was measured at 1.26g and occurred at the roof level. The next largest peak acceleration occurred at floor level 6 with a recorded peak acceleration of 1.13g. From the envelope of peak interstory drifts and accelerations, the influence of higher mode effects is apparent from the distribution of peaks.

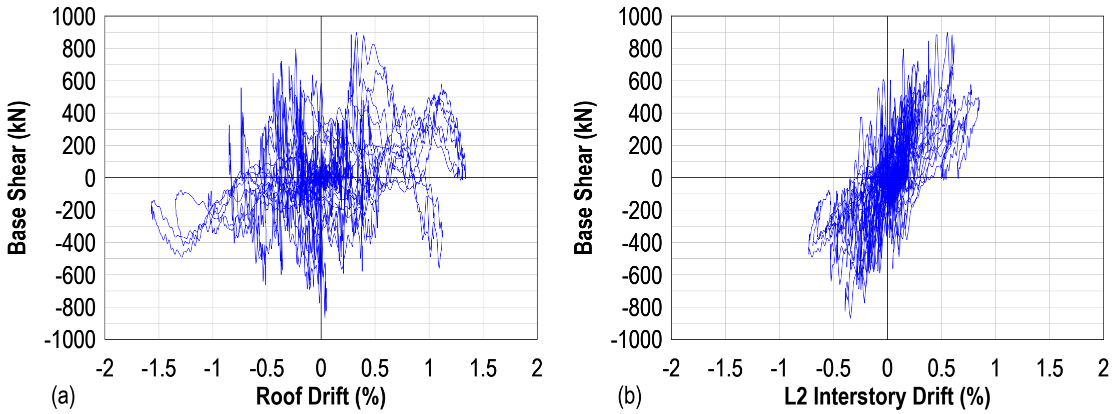

Figure 6. Loma Prieta (MCE$_R$): (a) Base shear vs. roof drift; (b) Base shear vs. level 2 interstory drift

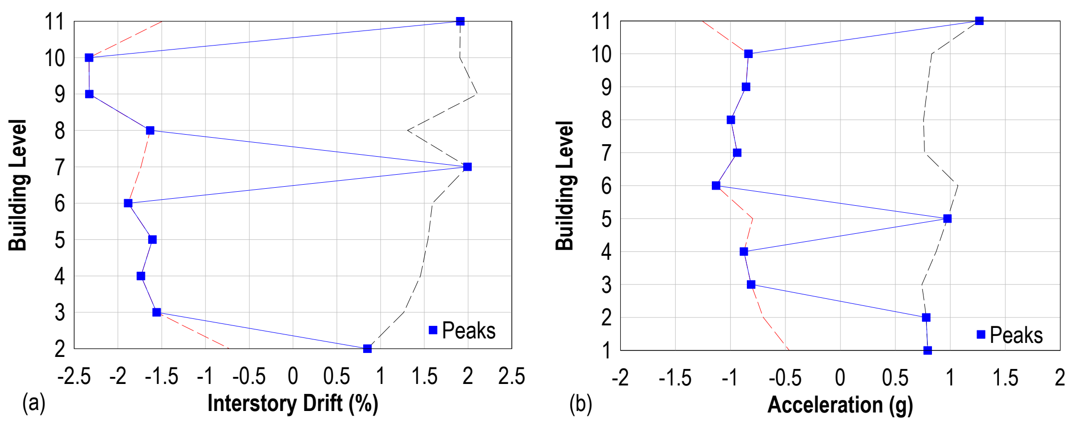

Figure 7. Loma Prieta (MCE$_R$): (a) Peak interstory drifts; (b) Peak level accelerations

4.3 Experimental Results – UFD Response

The UFD dampers are displacement controlled and are dependent on wall rocking behavior to produce wall uplift. To monitor wall uplift at the toe of the rocking walls, linear potentiometers were installed at these locations at each exterior and interior wall faces. Furthermore, the force response of the UFDs was obtained with 222 kN (50 kip) and 445 kN (100 kip) load washers installed on the thru-rods and uplift tension rods, respectively. Each UFD was detailed with 13 thru-rods, however, only load washers on 5 of the 13 rods at each UFD location were installed due to budgetary constraints. Accordingly, the results presented subsequently assumes an average tension force per thru-rod based on the average of the 5 load washers at each UFD location. On the contrary, load washers were installed at all the uplift tension rods (i.e., 8 locations). But it is noted that the uplift tension rod load washer at the North end of the West MPP wall, at the interior facing wall location, was damaged during instrumentation installation and consequently no data was collected on that sensor. The response plots presented subsequently support the following observations:

1. The hysteresis response of the damper 1 (i.e., south end of the West MP wall) is presented in Figure 8a in terms of the axial tension force measured in the uplift anchor rods and the net vertical displacement of the horizontal and vertical wedges. The latter was obtained as the difference between the measured displacement of the vertical string potentiometers attached to the respective vertical and horizontal wedges and represents the relative sliding motion between the UFD wedges. The following observations can be made:
    a. The UFDs are providing energy dissipation through observed presence of hysteresis loops. Compared to a rectangular hysteresis curve of flat slider friction devices, the differences in shape of the UFD hysteresis response observed here are due to the use of the combination

of inclined friction interfaces and use of disc-washers to provide the normal clamping forces. This has the effect of leading to a tapered rectangular hysteresis loop(s). Additionally, it is observed that the net vertical displacement returns to essentially zero indicating that there is negligible residual relative displacement between the two wedges of the UFD post-event.

b. The hysteresis response is not fully symmetrical on each side of the UFD (as would be expected for analytical and numerical models that assume idealized behavior of the UFD wedges as rigid blocks). This suggests that some differences can be expected due to installation fit-up (e.g., leading to binding from other sources of friction within the actual connection), differences in surface conditions within same friction plates (e.g., local as-delivered surface variations within the SS plates and LTB plates), and differences in forces in the tension anchor rods (on account of the aforementioned).

c. The net vertical displacement peaks between the West and East sides of the UFD do not match. That is the net vertical displacement is larger for the SE side of the UFD compared the SW side. This suggests that some unbalance of the wedges on opposite sides of the UFD can occur. However, the difference between the peak is approximately 1.5 mm (0.06 in.) which is a relatively small difference and does not appear to have any detrimental effects on the damper performance.

2. The coefficient of friction (COF) can be calculated through static force equilibrium of either the horizontal or vertical wedges with the measured horizontal clamping force and the corresponding measured tension force in the uplift anchor rods. Considering equilibrium of forces on the horizontal wedge, the calculated COF response history for damper 1 is presented in Figure 8b. At the southwest (SW) side of damper 1 the COF was determined to be in the range between 0.15 to (-)0.21. At the southeast (SE) side of damper 1 the COF was determined to be in the range between 0.19 to (-)0.22.

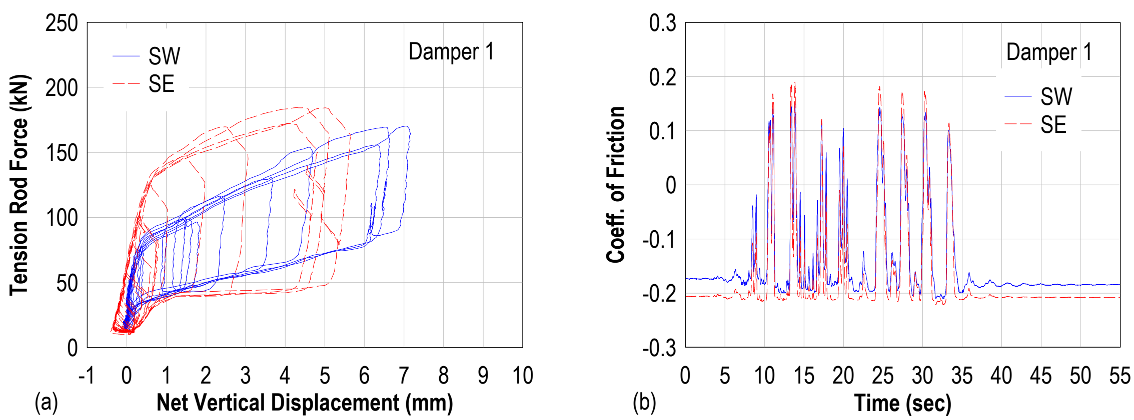

Figure 8. Loma Prieta (MCE_R): (a) Global UFD response; (b) COF response

5. Summary and Conclusions

The experimental results of a payload shake table test program of the NHERI TallWood 10-story mass timber building were presented. These payload tests were conducted after the completion of the test program of the NHERI TallWood project. The primary objective of these additional tests was to validate the performance of a proposed uplift friction damper (UFD) solution for mass timber rocking wall seismic-force resisting systems subjected to simulated earthquakes on a test building with realistic boundary conditions. A total of 10 earthquake tests of varying seismic hazard intensities, including an earthquake at the MCE_R level were conducted. Upper bound results reported using the MCE_R ground motion test showed that the post-tensioned mass timber rocking walls exhibited excellent seismic performance. Structural damage was limited to only the UFPs and functioned properly as structural fuses that could be replaced post-event without affecting the building's gravity frame system if deemed necessary in an actual significant earthquake scenario. Furthermore, these tests validated the performance of the UFDs subjected to earthquake loadings. For this test building, the UFDs were installed as added supplemental energy dissipating devices to the UFPs. The combination of UFP structural fuses attached to the boundary columns along the height of the building in parallel with the proposed

UFDs attached to the base of the rocking walls was shown to be an effective combination, leveraging the full potential of the natural kinematics of the rocking walls. The experimental results presented provide further evidence that tall mass timber buildings with post-tensioned rocking wall SFRSs is achievable.

6. Acknowledgements

Funding for these payload tests was provided by the National Science Foundation under award number CMMI 2025449. The authors would like to thank the NHERI TallWood Team for their support in being part of this test program. Additionally, Simpson Strong-Tie donated all the threaded rods and self-tapping screw hardware for the damper installation and their support is greatly appreciated. Thank you to Steve Pryor at Simpson Strong-Tie for assisting with this. Furthermore, the authors would like to thank graduate students Prashanna Mishra and Sir Lathan Wynn of the NHERI TallWood team for their help with installation of the dampers. Any opinions, findings, conclusions, and recommendations presented in this paper are those of the authors and do not necessarily reflect the views of the sponsors.

7. References

Akbas, T., R. Sause, J. M. Ricles, R. Ganey, J. Berman, S. Loftus, J. D. Dolan, S. Pei, J. W. van de Lindt and H.-E. Blomgren (2017). "Analytical and experimental lateral-load response of self-centering posttensioned CLT walls." Journal of Structural Engineering **143**(6): 1-15.

ASCE (2017). Minimum design loads and associated criteria for buildings and other structures : ASCE/SEI 7-16.

Blomgren, H.-E., S. Pei, Z. Jin, J. Powers, J. D. Dolan, J. W. van de Lindt, A. R. Barbosa and D. Huang (2019). "Full-Scale Shake Table Testing of Cross-Laminated Timber Rocking Shear Walls with Replaceable Components." Journal of Structural Engineering **145**(10): 1-14.

Bruneau, M. and G. MacRae (2017). "Reconstructing Christchurch: A seismic shift in building structural systems." The Quake Centre, University of Canterbury, Christchurch.

Council, I. C. (2015). International building code, Falls Church, Va. : International Code Council, 2015.

Filiatrault, A., R. Tremblay and R. Kar (2000). "Performance evaluation of friction spring seismic damper." Journal of Structural Engineering **126**(4): 491-499.

Ganey, R., J. Berman, T. Akbas, S. Loftus, J. D. Dolan, R. Sause, J. Ricles, S. Pei, J. v. d. Lindt and H.-E. Blomgren (2017). "Experimental Investigation of Self-Centering Cross-Laminated Timber Walls." Journal of Structural Engineering **143**(10): 1-14.

Green, M. and E. Karsh (2012). "The case for tall wood buildings." Canadian Wood Council on behalf of the Wood Enterprise Coalition by Forestry Innovation Investment, North Vancouver, BC, Canada.

Hashemi, A., P. Zarnani, R. Masoudnia and P. Quenneville (2018). "Experimental testing of rocking cross-laminated timber walls with resilient slip friction joints." Journal of Structural Engineering **144**(1): 1-16.

Iqbal, A., S. Pampanin, A. Palermo and A. Buchanan (2015). "Performance and design of LVL walls coupled with UFP dissipaters." Journal of Earthquake Engineering **19**(3): 383-409.

Kelly, J. M., R. Skinner and A. Heine (1972). "Mechanisms of energy absorption in special devices for use in earthquake resistant structures." Bulletin of NZ Society for Earthquake Engineering **5**(3): 63-88.

Kramer, A., A. R. Barbosa and A. Sinha (2016). "Performance of steel energy dissipators connected to cross-laminated timber wall panels subjected to tension and cyclic loading." Journal of Structural Engineering **142**(4): 1-10.

Loo, W. Y., P. Quenneville and N. Chouw (2016). "Rocking timber structure with slip-friction connectors conceptualized as a plastically deformable hinge within a multistory shear wall." Journal of Structural Engineering **142**(4): 1-15.

Moehle, J., C. Barkley, D. Bonowitz, S. Karlinsky, J. Maffei and C. Poland "The Resilient City–A Way of Thinking about Preparedness, Mitigation, and Rebuilding."

Pei, S., J. W. van de Lindt, A. R. Barbosa, J. W. Berman, E. McDonnell, J. Daniel Dolan, H.-E. Blomgren, R. B. Zimmerman, D. Huang and S. Wichman (2019). "Experimental Seismic Response of a Resilient 2-Story Mass-Timber Building with Post-Tensioned Rocking Walls." Journal of Structural Engineering **145**(11): 1-15.

Pei, S., J. W. van de Lindt, J. Berman, K. Ryan, J. D. Dolan, S. Pryor, S. Wichman, A. Busch and R. Zimmerman (2023). Full-scale 3-D shake table test of a ten-story mass timber building. World Conference on Timber Engineering. Olso, Norway.

Pei, S., J. W. van de Lindt, M. Popovski, J. W. Berman, J. D. Dolan, J. Ricles, R. Sause, H. Blomgren and D. R. Rammer (2016). "Cross-Laminated Timber for Seismic Regions: Progress and Challenges for Research and Implementation." Journal of Structural Engineering **142**(4): 1-11.

Polastri, A., I. Giongo, A. Angeli and R. Brandner (2018). "Mechanical characterization of a pre-fabricated connection system for cross laminated timber structures in seismic regions." Engineering Structures **167**: 705-715.

Sarti, F., A. Palermo and S. Pampanin (2016). "Development and testing of an alternative dissipative posttensioned rocking timber wall with boundary columns." Journal of Structural Engineering **142**(4): 1-12.

Smith, T., F. Ludwig, S. Pampanin, M. Fragiacomo, A. Buchanan, B. Deam and A. Palermo (2007). Seismic response of hybrid-LVL coupled walls under quasi-static and pseudo-dynamic testing. 2007 New Zealand Society for Earthquake Engineering Conference, Palmerston North, New Zealand.

Tatar, A. and D. M. Dowden (2022). "Analytical and numerical investigation of a low-damage uplift friction damper for self-centering cross-laminated timber rocking walls." Engineering Structures **254**: 113836.

Trutalli, D., L. Marchi, R. Scotta and L. Pozza (2019). "Capacity design of traditional and innovative ductile connections for earthquake-resistant CLT structures." Bulletin of Earthquake Engineering **17**(4): 2115-2136.

van de Lindt, J. W., M. O. Amini, D. Rammer, P. Line, S. Pei and M. Popov (2020). "Seismic Performance Factors for Cross-Laminated Timber Shear Wall Systems in the United States." Journal of Structural Engineering **146**(9): 04020172.

van de Lindt, J. W., J. Furley, M. O. Amini, S. Pei, G. Tamagnone, A. R. Barbosa, D. Rammer, P. Line, M. Fragiacomo and M. Popovski (2019). "Experimental seismic behavior of a two-story CLT platform building." Engineering Structures **183**: 408-422.

Wichman, S., J. Berman, R. Zimmerman and S. Pei (2022). Lateral design of a 10-story building specimen with mass timber rocking walls. 12th National Conference on Earthquake Engineer, 12NCEE. Salt Lake City, UT.